

# In silico exploration of pyrocannabinoid interactions with key protein targets

Giovanni A. Ramirez<sup>1</sup>, Tesfay T. Tesfatsion<sup>1</sup>, Monica K. Pittiglio<sup>1</sup>, Kyle P. Ray<sup>1</sup>, Andrew Westerkamp<sup>2</sup>, Westley Cruces<sup>1\*</sup>

<sup>1</sup>Colorado Chromatography Labs, 21323 I-76 Frontage Rd Bldg 201, Hudson, CO 80642

<sup>2</sup>Real Isolates, 48 Dunham Rd STE 3000, Beverly MA 01915

\*Corresponding Author: [wes@coloradochromatography.com](mailto:wes@coloradochromatography.com) 303-835-3244

## Abstract

Cannabinoids, particularly those derived from cannabis, have attracted considerable attention in recent years for their therapeutic potential in treating various diseases and ailments. In this study, we identified cannabinoid byproducts that result from the combustion of cannabidiol (CBD) - henceforth referred to as pyrocannabinoids - and employed molecular docking simulations to investigate their interactions with key protein targets implicated in different physiological processes. Specifically, we focused on peroxisome proliferator-activated receptor gamma (PPAR- $\gamma$ ), p21-activated kinase 1 (PAK1), CB1, CB2, and GPR119 proteins, elucidating the binding modes and affinities of pyrocannabinoid byproducts to these receptors. This investigation was done in collaboration with Real Isolates LLC. Our findings revealed diverse ligand-protein interactions, with some pyrocannabinoids displaying favorable binding energies and stable ligand-protein complexes. However, variations in binding affinities across different proteins underscored the complex pharmacological profiles of the pyrocannabinoids. Furthermore, the prediction of adsorption, distribution, metabolism, excretion and toxicity (ADMET) properties highlighted both promising and concerning aspects of cannabinoid pharmacokinetics, emphasizing the need for thorough preclinical evaluation. Additionally, our investigation into potential metabolic sites using cytochrome P450 enzymes provided insights into cannabinoid metabolites. Overall, our study contributes to the understanding of pyrocannabinoid pharmacology and informs the rational design of pyrocannabinoid-based therapeutics. Further experimental validation is warranted to translate these findings into clinically relevant applications.

Keywords: *In silico*; Computational Chemistry; GPCR; Cannabinoids; CB1; CB2; ADMET

## 1. Introduction

Cannabinoids have garnered the attention of many scientists and pharmacologists in recent years, with the importance being focused on the primary constituents of cannabis such as delta-9-tetrahydrocannabinol (D9-THC), Cannabidiol (CBD), cannabinol (CBN), and even more recently delta-8-tetrahydrocannabinol (D8-THC), testing the uses of these cannabinoids to treat diseases and mental issues such as chronic pain, multiple sclerosis, epilepsy, amyotrophic lateral sclerosis, Parkinson's disease, Huntington's disease, post-traumatic stress disorder, anxiety, sleep, opioid use disorder, Tourette's syndrome, cancer and cancer-related illness, glaucoma, and inflammatory bowel disease [1,2]. With over 150 cannabinoids reported in the plant and a select few being investigated, countless others are left uninvestigated [3].

The introduction of recent bills allowing for companies to sell novel and untested cannabinoids, leaves consumers open to possible adverse effects and possible complications from inhalation or consumption of these cannabinoids, with the mass production of the cannabinoids [4], introduction of byproducts and unclean product can lead to harm. The identification of the cannabinoids and their binding pockets, with in-silico data contributes to pre-investigational biologic studies and toxicology studies of consumed cannabinoids, while providing pertinent information for medicinal and organic chemists for possible drug design of novel analogs to surpass parent scaffolds.

Though many cannabis products are consumed via inhalation, there is little information about the full spectrum of cannabinoids in the products, or the transformations that they undergo during combustion. There is also no information on their ADME properties and binding affinities. Westerkamp et al developed a system for mimicking the smoking of cannabinoids and isolating novel pyrocannabinoid byproducts [5]. Using this technology, their group has identified many compounds captured from heating CBD flower. The unique alkylation on CBND, OMeCBND, OMeCBN, OPropylCBN, and OPeCBN are not usually seen on the cannabinoid scaffold; there is also no pharmacological information on these compounds.

Due to the lack of biological information on these compounds, our group has docked them against 7 proteins which have cannabinoid like ligands to identify key ligand interactions, while also compiling ADMET information, and hypothesized p450 sites of metabolism. The contribution of providing in-silico information provides context in discerning possible interaction within selected proteins and contrasting with other cannabinoids to determine agonistic, or antagonistic effects on selected proteins to help design biological studies and design analogs to treat diseases and ailments [6].

## **2. Methods and Materials**

All Molecular docking experiments were achieved on Cybertron PC CLX 13th Gen Intel(R) Core(TM) i9-13900KF @ 3.00 GHz comprising 24 computing cores. Schrödinger Release 2023-3: Glide software was used as the docking program [7-10]. Protein/ligand preparation, in silico molecular docking, prediction of ADMET properties, and hypothesized P450 sites of metabolism were prepared according to methodology from Cruces et al [11].

### *2.1. Proteins and Ligands Preparation*

All Molecular docking experiments were achieved on CybertronPC CLX 13th Gen Intel(R) Core(TM) i9-13900KF @ 3.00 GHz comprising 24 computing cores. Schrödinger Release 2023-3: Glide software was used as the docking program [7-10]. Crystal structures of CB1, CB2, GPR119, PAK1, and PPAR- $\gamma$  were retrieved from the RCSB Protein Data Bank. CB1 [(PDB: 7V3Z), (PDB: 5U09), (PDB: 6KQI)]. CB2 [(PDB: 5ZTY)]. GPR119 [(PDB: 7WCM)]. PAK1 [(PDB: 5DFP)]. PPAR- $\gamma$  [(PDB: 2P4Y)].

The proteins were prepared and minimized using a protein preparation workflow tool on Schrödinger Protein Preparation Wizard [7-10]. The external water molecules and ions were removed. Polar Hydrogens were added. Missing side chains were filled using Epic and PROPKA. Het states were generated at pH 7.4 (+/- 2.0). Heavy atoms converged to RMSD 0.30Å. 3D structures of cannabinoids and hydrogenated cannabinoids were established in 2D sketcher which was then exported as an SDF file and imported and prepared using LigPrep, to form 3D conformers, including the various 3D chiral conformations. All structures underwent geometrical optimization using Release 2023-3: Jaguar software using density functional theory (DFT) calculation with B3LYP/6-31G as the basis set for the calculation to afford the minimized energy chemical structures. The structures were then docked using Release 2023-3: Glide software from Schrödinger.

## 2.2. Protein Structure validation

Homology modeling was performed to validate the structure of the optimized protein from PDB prior to molecular docking. A program called PROCHECK [12,13] was used to validate modeled proteins. PROCHECK generates a Ramachandran plot and assesses the atomic distances, surface area, bond angle, and torsion angles. The Ramachandran Plot was provided information on stable conformations of amino acid residues in term of phi ( $\phi$ ) and psi ( $\psi$ ) angels as well as allowed and disallowed region for amino acid residues in high resolution, non-homologous protein crystal structures. Plot points represented the torsion angles of amino acid residues in a three-dimensional protein model.

## 2.3. In Silico Molecular Docking

The grid parameter was generated covering the CB1 pockets for (PDB:7V3Z) [-42.91, -163.58, 306.7], (PDB:5U09) [126.7,118.85,147.7], (PDB:6KQI) [-25.98, -8.77, 40.11] for x,y,z coordinates. The ligand diameter midpoint box follows a 10Å x 10Å x 10Å x,y,z dimension. The grid parameter was generated covering the CB2 pockets for (PDB:5ZTY) [9.09, -0.17, -55.72] for x,y,z coordinates. The Ligand diameter midpoint box follows a 10Å x 10Å x 10Å x,y,z dimension. The grid parameter was generated covering the GPR119 pocket (PDB:7WCM) [126.7, 118.85, 147.7] for x,y,z coordinates. The ligand diameter midpoint box follows a 10Å x 10Å x 10Å x,y,z dimension. The grid parameter was generated covering the PAK1 pocket (PDB:5DFP) [13.58, 34.37, -15.61] for x,y,z coordinates. The ligand diameter midpoint box follows a 10Å x 10Å x 10Å x,y,z dimension. The grid parameter was generated covering the PPAR- $\gamma$  pocket (PDB:2P4Y) [35.4, -21.89, 39.56\_B] for x,y,z coordinates. The ligand diameter midpoint box follows a 10Å x 10Å x 10Å x,y,z dimension.

Prepared proteins were produced by the protein preparation workflow tool on the Maestro 13.8 interface of Schrödinger Protein Preparation Wizard [7-10]. Prime MM-GBSA (MMGBSA dG Bind (NS) and MMGBSA dG Bind) energy was calculated and displayed in Table 4-SI. MM/GBSA calculations were accomplished to estimate the relative binding energies of cannabinoids to the receptors.

#### *2.4. Prediction of ADMET Properties*

The ADMET properties of the 40 cannabinoids were performed using QikProp version 4.4 integrated into Maestro (Schrödinger, LLC, New York, 2015) which predicts the widest variety of pharmaceutically relevant properties: QPlogS (predicted aqueous solubility), QPlogHERG (Predicted IC50 value for blockage of HERG K<sup>+</sup> channels), QPPCaco (predicted apparent Caco-2 cell permeability. Caco2 cells are a model for the gut-blood barrier), QPlogBB (predicted brain/blood partition coefficient), and % Human Oral Absorption (Predicted human oral absorption in gastrointestinal tract on 0 to 100% scale). The calculated physicochemical descriptors are displayed in Table 5-SI. QikProp bases its predictions on the full 3D molecular structure and the global minimum energy conformer of each compound was used as input for ADMET properties.

From the use of Schrodinger modeling software, SwissADME [15-17] was used as well for the prediction of the pharmacokinetic and pharmacology profile to provide an in-depth validation of data.

#### *2.5. Hypothesized P450 Sites of Metabolism*

Schrodinger P450 site of metabolism software was used to perform calculations. CYP isoform 2C9 and 3A4(intrinsic reactivity) function was used to determine possible sites of metabolism (SOM).

### **3. Results and Discussion**

### 3.1. Ramachandran plots

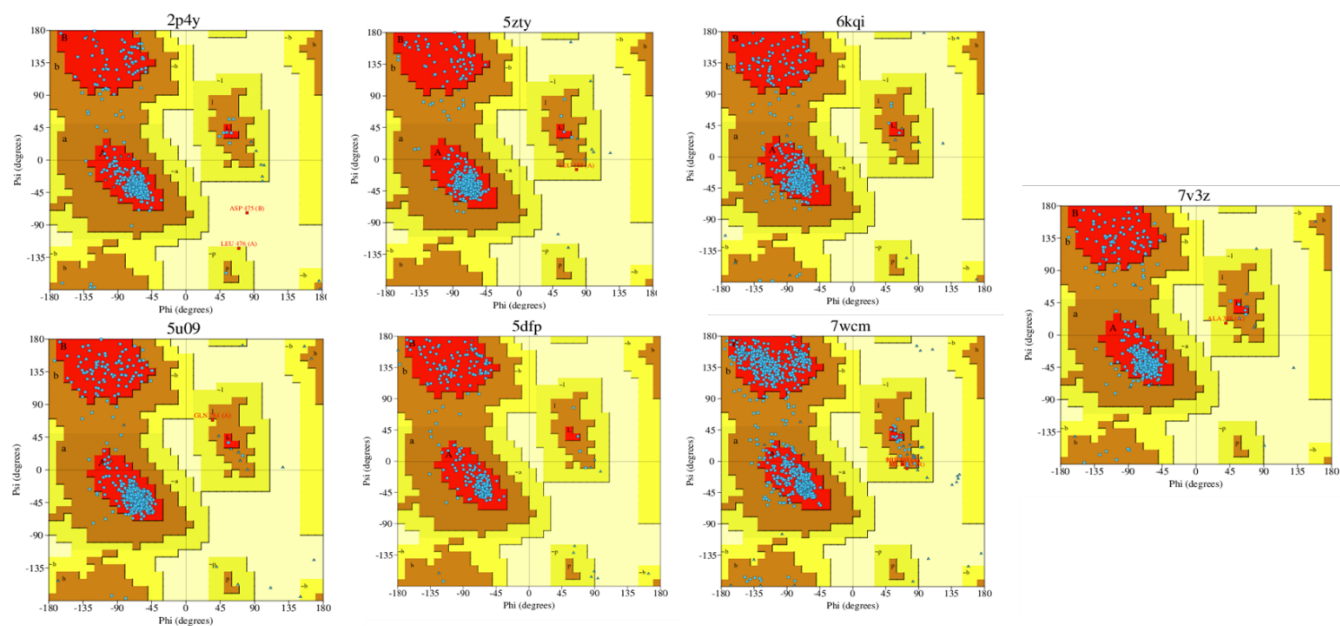


**Figure 1:** Using Procheck, proteins were verified prior to docking and minimization using Schrödinger.

2P4Y			5dfp			5u09		
	No. of residues	%-tage		No. of residues	%-tage		No. of residues	%-tage
Most favoured regions [A,B,L]	386	91.9%	Most favoured regions [A,B,L]	239	92.3%	Most favoured regions [A,B,L]	409	94.2%
Additional allowed regions [a,b,l,p]	32	7.6%	Additional allowed regions [a,b,l,p]	20	7.7%	Additional allowed regions [a,b,l,p]	24	5.5%
Generously allowed regions [-a,-b,-l,-p]	1	0.2%	Generously allowed regions [-a,-b,-l,-p]	0	0.0%	Generously allowed regions [-a,-b,-l,-p]	1	0.2%
Disallowed regions [XX]	1	0.2%*	Disallowed regions [XX]	0	0.0%	Disallowed regions [XX]	0	0.0%
Non-glycine and non-proline residues	420	100.0%	Non-glycine and non-proline residues	259	100.0%	Non-glycine and non-proline residues	434	100.0%
End-residues (excl. Gly and Pro)	14		End-residues (excl. Gly and Pro)	2		End-residues (excl. Gly and Pro)	2	
Glycine residues	18		Glycine residues	18		Glycine residues	29	
Proline residues	19		Proline residues	13		Proline residues	13	
Total number of residues	471		Total number of residues	293		Total number of residues	478	

5ZTY			6kqi			7v3z		
	No. of residues	%-tage		No. of residues	%-tage		No. of residues	%-tage
Most favoured regions [A,B,L]	385	94.4%	Most favoured regions [A,B,L]	379	88.8%*	Most favoured regions [A,B,L]	343	88.4%*
Additional allowed regions [a,b,l,p]	22	5.4%	Additional allowed regions [a,b,l,p]	48	11.2%	Additional allowed regions [a,b,l,p]	44	11.3%
Generously allowed regions [-a,-b,-l,-p]	1	0.2%	Generously allowed regions [-a,-b,-l,-p]	0	0.0%	Generously allowed regions [-a,-b,-l,-p]	1	0.3%
Disallowed regions [XX]	0	0.0%	Disallowed regions [XX]	0	0.0%	Disallowed regions [XX]	0	0.0%
Non-glycine and non-proline residues	408	100.0%	Non-glycine and non-proline residues	427	100.0%	Non-glycine and non-proline residues	388	100.0%
End-residues (excl. Gly and Pro)	2		End-residues (excl. Gly and Pro)	3		End-residues (excl. Gly and Pro)	4	
Glycine residues	23		Glycine residues	29		Glycine residues	28	
Proline residues	16		Proline residues	14		Proline residues	11	
Total number of residues	449		Total number of residues	473		Total number of residues	431	

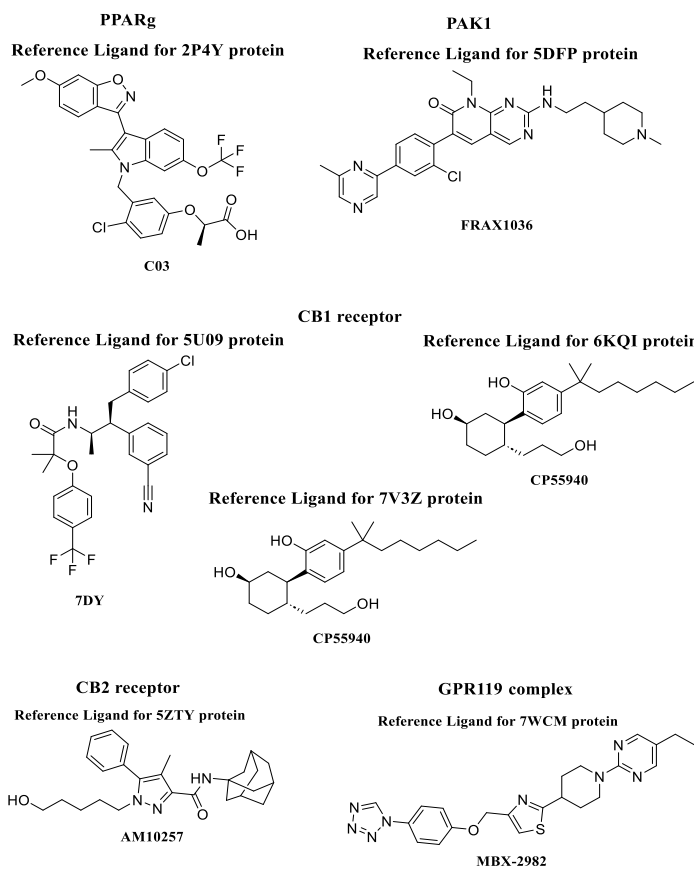
  

7wcm		
	No. of residues	%-tage
Most favoured regions [A,B,L]	852	91.2%
Additional allowed regions [a,b,l,p]	79	8.5%
Generously allowed regions [-a,-b,-l,-p]	3	0.3%
Disallowed regions [XX]	0	0.0%
Non-glycine and non-proline residues	934	100.0%
End-residues (excl. Gly and Pro)	16	
Glycine residues	68	
Proline residues	29	
Total number of residues	1047	

**Figure 2:** Procheck statistics of the verified proteins prior to docking.

Ramachandran plots serve as indirect verification tool of the stereochemistry and geometry of the complex by establishing that none of the geometries are in the forbidden electrostatically unfavored regions of the plot. The proteins identified above in figures 2 and 1 respectively identify 2P4Y, 5DFP, 5U09, 5ZTY, and 7WCM with the most favored regions having greater than 90% of the protein, within the A,B, and L regions. 6KQI, and 7V3Z are less than 90% with a larger percentage residing within the additional regions. The use of Ramachandran plots, are to validate the proteins prior to minimizations and docking of the chosen cannabinoids.

### 3.1. Molecular Docking of Cannabinoids



**Figure 3:** Reference ligands found within each docked protein. Reference ligands were used to identify the interacting residues.

2P4Y	5DFP	5U09	6KQI	7V3Z	5ZTY	7WCM
C03	FRAX1036	7DY	CP55940	CP55940	AM-10257	MBX-2982
agonist	PAK-1 Kinase inhibitor	inverse agonist	agonist	agonist	antagonist	agonist
SER142- HBOND	ASP106- HBOND	SER460- HBOND	ILE175- HBOND	ILE169- HBOND	H20-HBOND	TRP265- PI/CATION
	LEU99- HBOND	H <sub>2</sub> O- HBOND	SER81-HBOND	SER407- HBOND	TRP405- PHE116-Pi/Pi STACKING	TRP265-Pi/Pi STACKING
	H <sub>2</sub> O- HBOND		SER456- HBOND	LYS94-HBOND		PHE241-Pi STACKING
	GLU67- HBOND		PHE78- PHE176-Pi/Pi STACKING	SER75-HBOND		TRP238- Pi/CATION STACKING
				PHE72- PHE170-Pi/Pi STACKING		

**Table 1.** Ligands that were used as reference in the docking experiments, with each protein and their ligand activity when bound to respective protein, including the residue interaction of reference ligand.

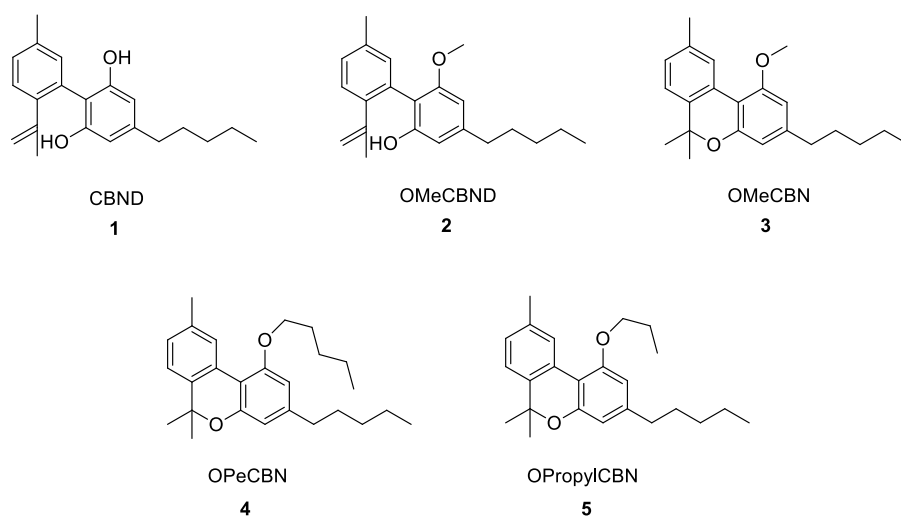


**Figure 4:** CBND, OMeCBND, OMeCBN, OPeCBN, OPropylCBN that were screened.

### 3.1.1. PPAR- $\gamma$ (2P4Y)

Compounds **1**, **2**, and **3** have ligand interactions with 2P4Y whereas **4** and **5** do not. The common interactions between compounds and protein are H-bonding. Compound **2** shows the best binding energy at -8.94 kcal/mol. Compounds **4** and **5** have binding energies of -5.29 and -7.30 respectively. Compound **2** has the most stable ligand-protein complex with relative binding-free energies of -61.08 kcal/mol and -54.68 kcal/mol. These findings suggest the potential of certain cannabinoids to modulate PPAR- $\gamma$  activity, which is involved in metabolic regulation and inflammation.

### 3.1.2. PAK1 (5DFP)

Compounds **1**, **2**, **4**, and **5** show ligand interactions with 5DFP and compound **3** does not. The interactions between the ligand and protein are H-bonding and  $\pi$ -stacking. Compound **2** has the lowest binding energy at -6.66 kcal/mol. Compound **2** is also the most stable ligand-protein complex with relative binding-free energies of -58.92 kcal/mol and -45.88 kcal/mol. This suggests the potential of certain cannabinoids as inhibitors or modulators of PAK1, a kinase implicated in cancer progression and cellular signaling pathways.

### 3.1.3. CB1 (5U09, 6KQI, 7V3Z) and CB2 (5ZTY)

Compounds **1**, **2**, and **5** show ligand interactions with 5U09. The interactions between the ligand and protein are H-bonding and  $\pi$ -cation. Compound **2** has the lowest binding energy at -10.63 kcal/mol. However, compound **5** has the most stable ligand-protein complex with relative binding-free energies of -87.92 kcal/mol and -75.94 kcal/mol.

All five compounds show ligand interactions with 6KQI. The interactions between the ligand and protein are H-bonding and  $\pi$ -stacking. Compound **4** has the lowest binding energy at -9.75 kcal/mol. Compound **5** is the most stable ligand-protein complex with relative binding-free energies of -69.21 kcal/mol and -50.64 kcal/mol.



All five compounds show ligand interactions with 7V3Z. The interactions between the ligand and protein are H-bonding and  $\pi$ -stacking. Compound **1** has the lowest binding energy at -10.66 kcal/mol. Compound **2** is the most stable ligand-protein complex with relative binding-free energies of -71.00 kcal/mol and -51.80 kcal/mol.

All five compounds show ligand interactions with 5ZTY. The interactions between the ligand and protein are H-bonding and  $\pi$ -stacking. Compound **4** has the lowest binding energy at -10.44 kcal/mol. Compound **4** is also the most stable ligand-protein complex with relative binding-free energies of -77.48 kcal/mol and -63.08 kcal/mol.

Our results revealed diverse interactions between cannabinoids and both CB1 and CB2 receptors, including hydrogen bonding and  $\pi$ -stacking interactions. Compound **2** exhibited the lowest binding energy (-10.63 kcal/mol) with CB1, indicating a strong affinity. Interestingly, compound **5** formed the most stable ligand-protein complex with CB2. These findings suggest the potential of cannabinoids to modulate cannabinoid receptors, which play crucial roles in pain modulation, appetite regulation, and immune function.

#### 3.1.4. GPR119 (7WCM)

Compounds **1**, **2**, **4**, and **5** show ligand interactions with 7WCM and compound **3** does not. The interactions between the ligand and protein are H-bonding and  $\pi$ -stacking. Compound **1** has the lowest binding energy at -9.38 kcal/mol. Compound **1** is also the most stable ligand-protein complex with relative binding-free energies of -45.03 kcal/mol and -39.51 kcal/mol. These results suggest the potential of cannabinoids to modulate GPR119, a receptor implicated in glucose homeostasis and insulin secretion [18].

### 3.2. In Silico ADMET Properties of Pyrocannabinoids

The predicted ADMET properties and descriptors for the compounds are presented in Table 2. The aqueous solubility (QPlogS) is critical for the estimation of absorption and distribution of the compounds within the body and ranges between -5.45 and -11.05. A majority of the tested cannabinoids have solubility values out of the recommended range (compounds **2**, **3**, **4**, **5**). Cannabinoids with the ether functional group displayed poor solubility. QPlogHERG is another parameter that is out of the recommended range for compounds **1**, **2**, **4**, **5**. It is predicted that at half-maximal inhibition, HERG K channel blockage can lead to arrhythmia and cardiac adverse events [19]. Most other descriptors are within the recommended range by QikProp ADMET software for 95% of known oral drugs [7-10]. These results suggest that some of the tested cannabinoids exhibited acceptable physiochemical properties. These findings underscore the importance of thorough preclinical evaluation to ensure the safety and efficacy of novel cannabinoids before clinical use. Figure 5 and 6 below visualizes the physiochemical characteristics of the pyrocannabinoids. In a previous study [20], non-clinical safety study was conducted on hydrogenated derivatives, with the cannabinoids failing hERG, but passing the Nav/Cav repolarization testing, passing the cardiac safety assessment.

**Table 2:** General ADMET Bio Scores, generated by Schrödinger software.

Compound	MW	QLogS <sup>a</sup>	QLogHERG <sup>b</sup>	QPPCaco <sup>c</sup>	QLogBB <sup>d</sup>	% Human Oral Absorption <sup>e</sup>
<b>1</b>	310.43	-5.45	-5.14	2146.77	-0.61	100.00
<b>2</b>	324.46	-6.51	-5.25	4957.34	-0.24	100.00
<b>3</b>	324.46	-8.50	-4.88	9906.04	0.53	100.00
<b>4</b>	380.56	-11.05	-5.63	9906.04	0.78	100.00
<b>5</b>	352.51	-9.56	-5.09	9906.04	0.65	100.00

Range of 95% drugs: a) Predicted aqueous solubility [-6.5 to +0.5]; b) HERG K<sup>+</sup> Channel Blockage (log IC<sub>50</sub>) [concern below -5]; c) Apparent Caco-2 cell permeability in nm/s [<25 poor; >500 excellent]; d) Predicted log of the blood/brain partition coefficient [-3.0 to +1.2]; e) Human Oral Absorption in GI [<25% is poor].

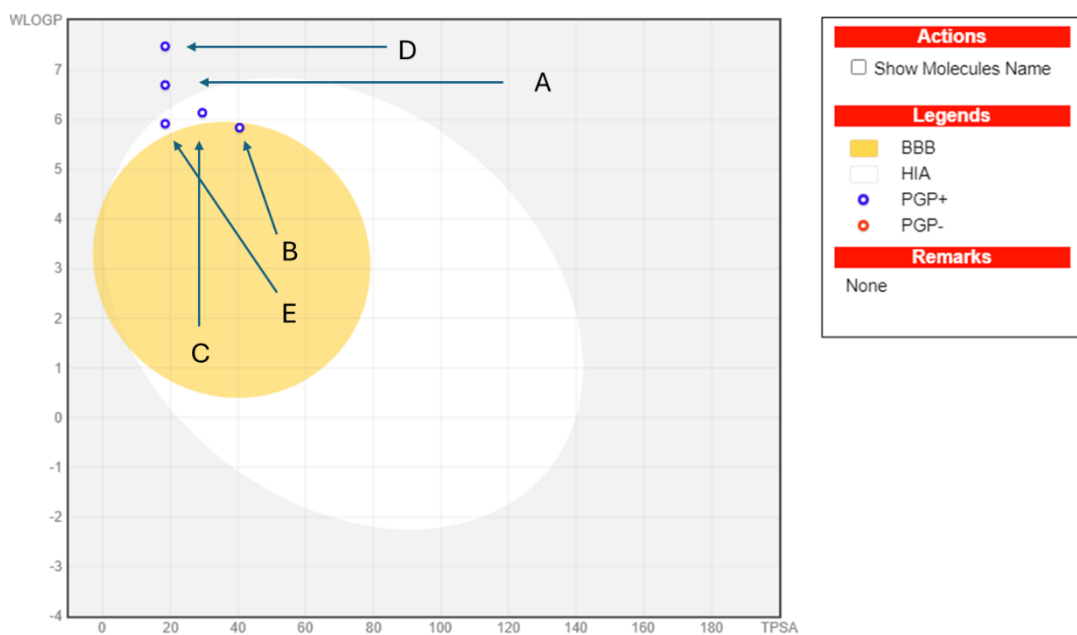
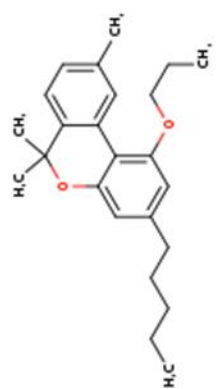
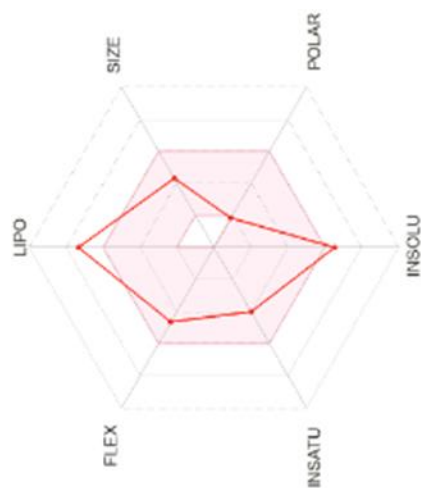
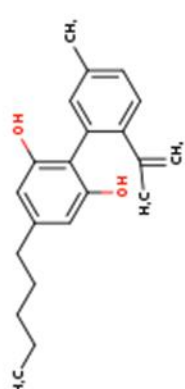
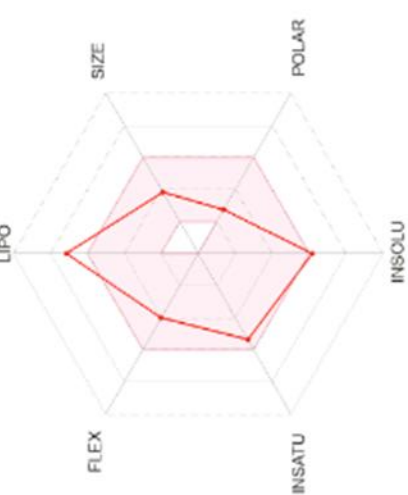


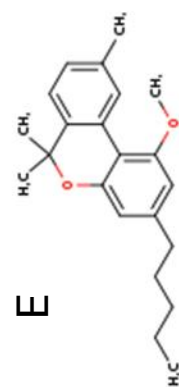
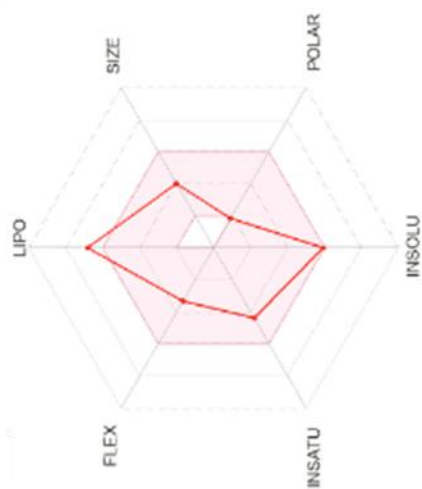
**Figure 5:** Boiled egg graph identifies their properties. BBB-blood brain barrier, HIA-human intestinal absorption, [PGP+/PGP-]-dictates the if there is effect on the central nervous system or not.



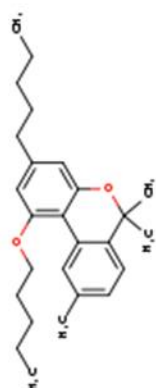
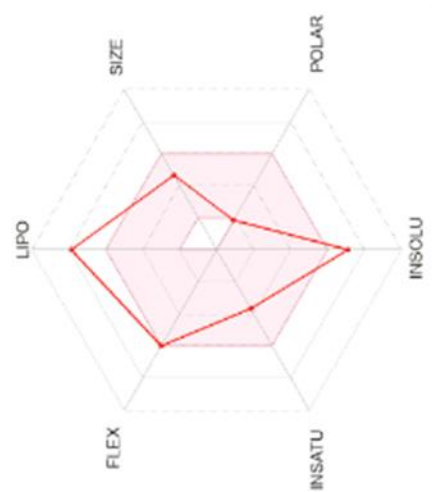
A



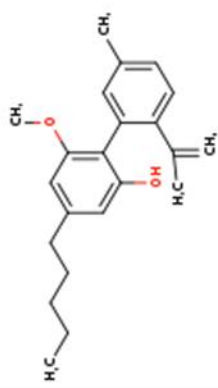
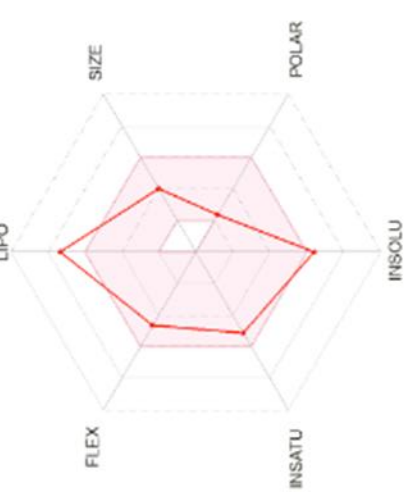
B



E



D



C

**Figure 6:** the various cannabinoids with their given SWISSADME profile visualizing their physiochemical characteristics.

The score of the pyrocannabinoids generated by Schrödinger, are similar to the scores generated by SWISSADME [15-17] as shown in SI figure 3 and 4. The use of these software generates usable pharmacodynamic and physiochemical scores that describe the compounds properties, which is of importance and interest when identifying support for the synthesis of analogs treating diseases where the physicochemical characteristics can either increase or decrease efficiency of the drugs towards their desired targets. All cannabinoids as shown above in figure 6, are lipophilic and insoluble which although they pass the Lipinski rule of 5 minus one rule, challenges would need to be overcome which studies of making cannabinoids water soluble have been conducted [21].

### 3.3. *In Silico* Identification of Metabolic Sites of Pyrocannabinoids Using Cytochrome P450

CYP isoforms 2C9 and 3A4 were chosen as models because they are key components in the reported metabolism routes of major cannabinoids [22]. using 2C9 as shown in figure 7a below, the green dots identify interactions with the 2C9 enzyme where possible oxidation may occur. While shown in figure 7b, the oxidative sites predicted for the isoenzyme 3A4 are as shown. Further possible products of oxidation are shown in SI Figure 3 and 4.

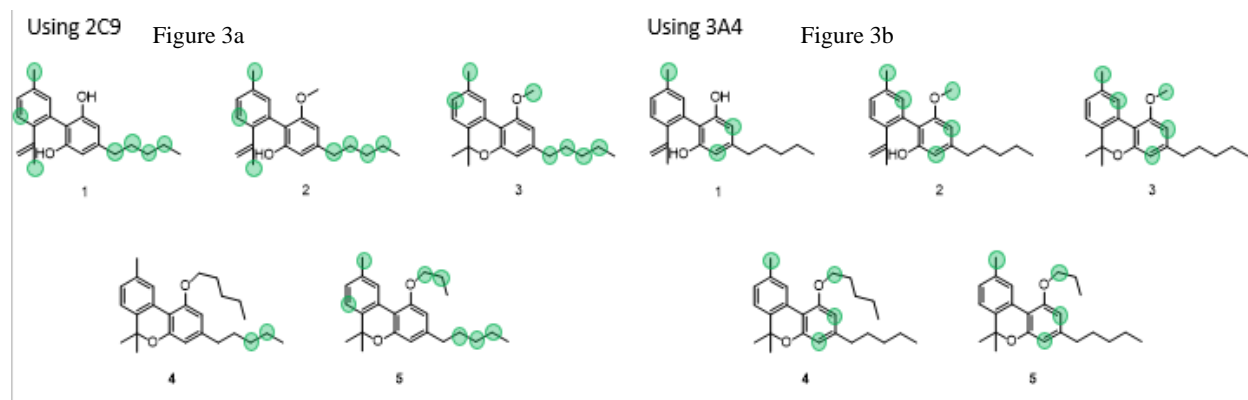


**Figure 7a-b:** The predicted sites of metabolism on the tested compounds are highlighted by the green circles, according to the isoform enzyme.

## 4. Conclusion

In conclusion, our study delved into the molecular properties and pharmacological potential of various cannabinoids present in cannabis smoke, shedding light on their interactions with key protein targets, ADMET properties, and potential metabolic pathways. Through molecular docking experiments, we elucidated the binding modes and affinities of smoked CBD flower products to PPAR- $\gamma$ , PAK1, CB1, CB2, and GPR119 proteins, providing insights into their agonist or antagonist effects. Our findings reveal intriguing ligand-protein interactions, with some cannabinoids exhibiting favorable binding energies and stable ligand-protein complexes.

However, it's crucial to acknowledge the diversity in interactions across different proteins, suggesting a nuanced pharmacological profile for each cannabinoid. Furthermore, the prediction of ADMET properties highlighted both promising and concerning aspects of cannabinoid

pharmacokinetics. While some cannabinoids demonstrated acceptable physicochemical properties, others raised concerns regarding aqueous solubility and potential cardiac adverse events due to HERG channel blockage. These insights underscore the importance of rigorous preclinical evaluation to ensure the safety and efficacy of novel cannabinoids before clinical use.

Overall, our study contributes to the growing body of research aimed at harnessing the therapeutic potential of cannabinoids while addressing safety concerns and optimizing drug development strategies. By combining computational modeling with experimental validation, we pave the way for the rational design of cannabinoid-based drugs for the treatment of various diseases and ailments. However, further studies, including in vitro and in vivo experiments, are warranted to validate our findings and translate them into clinically relevant applications.

## **Author Information**

### **ORCID**

Giovanni Ramirez: <https://orcid.org/0000-0002-3716-862X>

Tesfay Tesfatsion: <https://orcid.org/0000-0002-3743-9522>

Monica Pittiglio: <https://orcid.org/0009-0007-1044-7614>

Kyle Ray: <https://orcid.org/0000-0001-5648-0099>

Westley Cruces: <https://orcid.org/0000-0003-3023-7626>

### **Abbreviations**

ADMET: adsorption, distribution, metabolism, excretion and toxicity

CBD - cannabidiol

PAK1 - p21-activated kinases

PPAR- $\gamma$  - peroxisome proliferator-activated receptor gamma

### **Declarations**

### **Ethical Approval**

Not applicable

### **Funding Statement**

There is no funding to report.

### **Availability of Data and Materials**

All data has been provided in the Supplemental information.

## Author Contributions

Conceptualization: GAR, AW, WC. Methodology: GAR, WC. Data Analysis: GAR, TTT, WC. Computational Modeling: GAR. Writing – Original Draft: GAR, WC. Writing – Revision and Editing: GAR, TTT, MKP, WC. Supervision: WC. Project Administration: KPR, WC.

## Author Confirmation

All authors have read and approved this manuscript for submission.

## Author Disclosure

GAR, TTT and MKP are employees of Colorado Chromatography Labs. WC and KPR are founders of Colorado Chromatography Labs. AW is the founder of Real Isolates.

## References

1. C. A. Legare, W. M. Raup-Konsavage, K. E. Vrana, Therapeutic potential of cannabis, cannabidiol, and cannabinoid-based pharmaceuticals, *Pharmacology*, 2022, 107 (3-4), 131-149, <https://doi.org/10.1159/000521683>
2. S. K. Bhamra, A. Desai, P. Imani-Berendjestanki, M. Horgan, The emerging role of cannabidiol (CBD) product; a survey exploring the public's use and perceptions of CBD. *Phytotherapy Research*, 2021, 35 (10) 5734-5740 <https://doi.org/10.1002/ptr.7232>
3. L. O. Hanus, S. M. Meyer, E. Munoz, O. Tagliatalata-Scafati, G. Appendino Phytocannabinoids: a unified critical inventory, *Nat Prod Rep* 2016, 33, 1357 <https://doi.org/10.1039/c6np00074f>
4. Docampo-Palacios, M. L., Ramirez, G. A., Tesfatsion, T. T., Pittiglio, M. K., Ray, K. P., Cruces, Comprehensive Safety Assessment of Diverse Cannabinoids: A Scientific Inquiry, 2024, <https://doi.org/10.21203/rs.3.rs-3934959/v1>
5. C. M. Shields, A. M. Westerkamp, Methods for obtaining compounds from a plant or fungus material, respective compositions, and uses thereof, US 2023/0295067A1, September 21, 2023
6. Iqbal, S., Matsabisa, M. In silico investigation of cannabinoids from Cannabis sativa leaves as a potential anticancer drug to inhibit MAPK-ERK signaling pathway and EMT induction. *In Silico Pharmacol.* 12, 41 (2024). <https://doi.org/10.1007/s40203-024-00213-4>
7. Bowers, K. J.; Chow, E.; Xu, H.; Dror, R. O.; Eastwood, M. P.; Gregersen, B. A.; Klepeis, J. L.; Kolossvary, I.; Moraes, M. A.; Sacerdoti, F. D.; Salmon, J. K.; Shan, Y.; Shaw, D. E., "Scalable algorithms for molecular dynamics simulations on commodity clusters", *Proceedings of the ACM/IEEE Conference on Supercomputing (SC06)*, Tampa, Florida, 2006, November 11-17

8. Johnston, R. C.; Yao, K.; Kaplan, Z.; Chelliah, M.; Leswing, K.; Seekins, S.; Watts, S.; Calkins, D.; Chief Elk, J.; Jerome, S. V.; Repasky, M. P.; Shelley, J. C., “Epik: pKa and protonation state prediction through machine learning”, *J. Chem. Theory Comput.* 2023, 19, 2380–2388
9. Ross, G. A., Lu, C., Scarabelli, G.; Albanese, S. K.; Houang, E.; Abel, R.; Harder, E. D.; Wang, L., “The maximal and current accuracy of rigorous protein-ligand binding free energy calculations”, *Commun. Chem.*, 2023, 6(222)
10. Friesner, R. A.; Banks, J. L.; Murphy, R. B.; Halgren, T. A.; Klicic, J. J.; Mainz, D. T.; Repasky, M. P.; Knoll, E. H.; Shaw, D. E.; Shelley, M.; Perry, J. K.; Francis, P.; Shenkin, P. S., “Glide: A new approach for rapid, accurate docking and scoring. 1. Method and assessment of docking accuracy”, *J. Med. Chem.*, 2004, 47, 1739–1749
11. Docampo-Palacios, M. L., Ramirez, G. A., Tesfatsion, T. T., Pittiglio, M. K., Ray, K. P., Cruces, W., *In Silico ADMET, binding affinities, and properties of hydrogenated cannabinoids*, *J. Theor. Comp. Sci.* 2024, 10(1), 1-12, <https://doi.org/10.35248/2376-130X.24.10.205>
12. Laskowski R A, MacArthur M W, Moss D S and Thornton J M (1993). PROCHECK: a program to check the stereochemical quality of protein structures. *J. Appl. Cryst.*, 26, 283-291.
13. Laskowski R A (1995). SURFNET: A program for visualizing molecular surfaces, cavities and intermolecular interactions. *J. Mol. Graph.*, 13, 323-330.
15. Daina, A., Michielin, O. & Zoete, V. SwissADME: a free web tool to evaluate pharmacokinetics, drug-likeness and medicinal chemistry friendliness of small molecules. *Sci Rep* 7, 42717 (2017). <https://doi.org/10.1038/srep42717>
16. Daina, A.; Michielin, O.; Zoete, V. ILOGP: A Simple, Robust, and Efficient Description of n-Octanol/Water Partition Coefficient for Drug Design Using the GB/SA Approach. *J. Chem. Inf. Model.* 2014, 54 (12), 3284–3301. <https://doi.org/10.1021/ci500467k>.
17. Daina, A.; Zoete, V. A BOILED-Egg to Predict Gastrointestinal Absorption and Brain Penetration of Small Molecules. *ChemMedChem* 2016, 11 (11), 1117–1121. <https://doi.org/10.1002/cmdc.201600182>.
18. Overton HA, Fyfe MC, Reynet C. GPR119, a novel G protein-coupled receptor target for the treatment of type 2 diabetes and obesity. *Br J Pharmacol.* 2008;153(51):576-581
19. Creanza, T. M.; Delre, P.; Ancona, N.; Lentini, G.; Saviano, M.; Mangiatordi, G. F. Structure-Based Prediction of hERG-Related Cardiotoxicity: A Benchmark Study. *J. Chem. Inf. Model.* 2021, 61 (9), 4758–4770. <https://doi.org/10.1021/acs.jcim.1c00744>.
20. Tesfatsion, T. T., Ramirez, G. A., Docampo, M. L., Collins, A. C., Ray, K. P., Cruces, W., Evaluation of In-Vitro Cytotoxicity, Genotoxicity and Cardiac Safety of Hydrogenated Cannabidiol on Cells Using Metabolic Assay, AMES and hERG Test, *Pharmacogn. Mag.*, 2023, <https://doi.org/10.1177/09731296231195941>
21. Pertwee, R. G.; Gibson, T. M.; Stevenson, L. A.; Ross, R. A.; Banner, W. K.; Saha, B.; Razdan, R. K.; Martin, B. R. O-1057, a Potent Water-soluble Cannabinoid Receptor Agonist with

Antinociceptive Properties. *Br. J. Pharmacol.* 2000, 129 (8), 1577–1584.  
<https://doi.org/10.1038/sj.bjp.0703245>.

22. Lucas, C. J.; Galettis, P.; Schneider, J. The Pharmacokinetics and the Pharmacodynamics of Cannabinoids. *Br. J. Clin. Pharmacol.* 2018, 84 (11), 2477–2482.  
<https://doi.org/10.1111/bcp.13710>.